Efficiency of channel codes for different fading models in 5G enhanced mobile broadband scenario

Mikhail Khmelevsky[1], Gennady Kazakov[2]

[1]Department of Networks and Communication Systems, Moscow Technical University of Communications and Informatics, Moscow, Russia

[2]Department of Theoretical Radio Engineering, Moscow Aviation Institute (National Research University), Moscow, Russia

Article Info

ABSTRACT

In urban environments, 5th generation (5G) signals are subject to interference, multiple propagation and thermal noise, resulting in a significant amount of errors. In this regard, channel coding is applied, which allows to increase the reliability of the transmitted message. This work focuses on comparing the performance of low-density parity check (LDPC) and polar codes standardized by the 3rd generation partnership project (3GPP) for application in 5G networks in physical downlink shared channel (PDSCH) under multipath propagation conditions in enhanced mobile broadband (eMBB) scenario. The performance of the codes under study was investigated considering all signal processing operations implemented in hardware in 5G channels. We used clustered delay line (CDL) and tapped delay line (TDL) models as propagation channel models. Channel configuration and selection of signal parameters were based on the analysis of commercially launched 5G networks. One of the simulations results we observed was the high signal-to-noise ratio (SNR) required to transmit the signal while ensuring a given block error rate (BLER). Polar codes demonstrated both a gain in coding over LDPC codes and a loss in decoding delay of the received signal due to a more complex decoding algorithm.

Corresponding Author:

Gennady Kazakov
Department of Theoretical Radio Engineering, Moscow Aviation Institute (National Research University)
Volokolamskoe Shosse 4, 125993 Moscow, Russia
Email: jee2@mail.ru

1. INTRODUCTION

The 5th generation new radio (5G NR) technology is rapidly evolving and improving its bandwidth, energy efficiency and flexibility in order to provide users with a larger set of services and applications. International Telecommunication Union (ITU) recommendation M.2083 [1] has defined three 5G application scenarios: enhanced mobile broadband (eMBB), massive machine type communications (mMTC) and ultra-reliable and low latency communications (URLLC). Thus, for eMBB, the important metric is the ultimate transmission speed; URLLC requires low latency (less than 1 ms) and extremely high reliability (99.999%); mMTC emphasizes high connectivity density and device energy efficiency. In the current phase of 5G deployment, the focus is on the eMBB usage scenario. High-speed and high-quality multimedia services like virtual reality (VR), augmented reality (AR), high-resolution video are available to users through the eMBB services. The eMBB scenario should support a wide range of code rates, different code lengths and modulation orders.

Compared to 4th generation long-term evolution (4G LTE), the distinctive feature of 5G NR is the use of two new error-correcting channel codes. Low-density parity check (LDPC) codes have replaced turbo

codes in user data channels and polar codes have replaced tail-biting convolutional codes (TBCC) in control channels to improve data rate and provide acceptable error correction performance [2]. LDPC, turbo codes and polar codes have similar channel performance for data intensive applications, while LDPC is less complex to implement. The system's performance is improved over other modern channel codes (TBCC and turbo codes) when combining cyclic redundancy check (CRC) codes with polar codes that are decoded using the successive cancellation list (SCL) algorithm. Nevertheless, polar coding is less efficient than LDPC for high data rates.

The main goal of this work was to compare the performance of the selected channel codes under physical downlink shared channel (PDSCH) signal and environmental parameters approximating those realized by the leading operators of 5G communication networks. From this, it is possible to derive estimations of the signal-to-noise ratio (SNR) values that are more likely to be experienced by users from 5G systems. As compared to the signal parameters that have been arbitrarily established by other researchers.

This paper presents an evaluation of the performance of polar and LDPC codes in a PDSCH channel for several information block sizes. We would like to emphasize that this study of selected codes has been performed considering all signal processing operations performed in 5G physical channels. In our work, we used multipath propagation channel models such as tapped delay line (TDL) and clustered delay line (CDL). The application of these models allows us to obtain SNR estimates closer to the real ones than when using Rice/Reilly channels. TDL-A and CDL-A channels were used in the case of line of sight (LOS), TDL-D and CDL-D in the case of non-line-of-sight (NLOS). The comparison was made on the target parameter of block error rate (BLER) from the symbol SNR.

In recent years, many observed a sharp increase in research devoted to the study of the effectiveness of LDPC and polar codes, as well as the search for efficient encoders and decoders that can provide a compromise between the required high performance and throughput and low hardware complexity, cost and power consumption. For example, Hui et al. [3] describes LDPC and polar codes adopted by the standard and 5G NR, the peculiarities of their application. The performance advantages of the newly applied codes are compared with the characteristics of the codes used in the long-term evolution (LTE). A comprehensive review of the main channel codes adopted since the third generation of mobile communications is presented in the book [4], where the results of the study of their application performance are also presented. Richardson and Kudekar [5] reviewed the channel code requirements for 5G NR. Innovations in LDPC codes that fulfil the requirements of 5G NR are presented and explained.

Efficiency of channel codes application is analyzed in [6], where dependences of block transmission error probabilities on symbol signal-to-noise ratio are presented for a number of sets of coding methods (turbo codes, polar codes and LDPC) and code-modulation schemes at average codeword length (about thousands of bits). Čarapić et al. [7] conducted compared simulation studies on the use of LDPC and polar codes for message transmission through various channel models like the additive white Gaussian noise (AWGN) channel, Rice and Rayleigh models. The simulation results reflect the characteristics of LDPC and polar codes in the case of channel models: AWGN channel without fading and AWGN channel with fading. In [8], an overview of the coding/decoding process in 5G NR is given and a comparison of the applied codes is made through bit error rate (BER) and BLER performance. Tahir et al. [9] examines how convolutional codes, turbo codes, LDPC codes, and polar codes perform in terms of bit error rate for multiple application scenarios with varying information block lengths and code rates. Comparative analysis of performance of advanced turbo codes with list decoding and polar codes with support of CRC codes with list decoding under AWGN conditions for short blocks of information at low code rates using BLER as a measure of efficiency is presented in [10]. Cuc et al. [11] performed a comparative analysis of LDPC and polar codes in terms of their performance, defined by analyzing BER versus SNR in AWGN channel.

The task of many works was to evaluate and compare the effectiveness of using one or more coding technologies in the communication system of a certain type or standard. For example, El-Ebbasy et al. [12] considered the possibility of using polar codes with SCL decoders in digital video broadcasting (DVB) systems, compared the efficiency of polar codes and LDPC codes in terms of BER, encoder/decoder delay and throughput. The BLER metric was used in [13] to evaluate different channel coding methods that can be implemented in Institute of Electrical and Electronics Engineers (IEEE) standard 802.11b. Among the merits of the work are both the consideration of actual coding techniques used in other standards (5G NR polar code and LTE turbo codes) and the comparison of efficiency based on simulation results under different propagation channel models.

The authors of a large number of articles devoted to the peculiarities and efficiency of channel coding application in 5G NR networks dwell on a specific scenario or application area. For example, Chatzoulis et al. [14] studied and evaluated the effectiveness of 5G NR turbo codes, polar codes and LDPC codes on the quality of service (QoS) under the environment parameters characteristic of the vehicle-to-everything (V2X) communication system. Thus, in addition to evaluating a number of coding schemes and modeling scenarios based on the frame error rate (FER) parameter (similar to BLER), the researchers studied

a set of other parameters (minimum required SNR, and transmit power) necessary to realize QoS of a certain quality. In the paper [15], based on the characteristics of block error rate (BLER) and computational complexity, the effectiveness of a number of channel coding schemes (turbo, LDPC codes, polar and convolutional codes) for URLLC scenario in 5G NR is investigated. In [16], a study of polar code in eMBB 5G NR scenario was carried out for both Uplink and downlink control information (UCI and DCI) signals and broadcast channel, in a transmission channel with AWGN. The results obtained were presented using the BER parameter. A similar study was conducted in [17], where in the case of a 5G NR downlink line system for different quadrature amplitude modulation (QAM) schemes, the effectiveness of applying the orthogonal time frequency space (OTFS) waveform to the orthogonal frequency-division multiplexing (OFDM) waveform was compared for TDL and CDL channel propagation models considering the application of minimum mean square error (MMSE) and decision feedback equalizers (DFE).

Cuc *et al*. [18] presented simulation results in the form of a number of BER characteristics related to turbo codes, LDPC codes and polar codes in a channel with additive white Gaussian noise in the presence of inter-symbol interference. Several types of equalizers (zero-forcing and MMSE) have been applied at the receiving end to eliminate the negative effects of interference. A number of studies [19]–[21] were devoted to comparing and analyzing the efficiency of channel codes (turbo codes, polar codes and others), mainly through the BER and BLER characteristics. In Shao *et al*. [22] reflected many aspects affecting the implementation complexity of turbo decoders, LDPC and polar decoders. Later, the throughput, error correction capability, flexibility, area efficiency and energy efficiency of implementation on application-specific integrated circuit (ASIC) were compared.

A detailed analysis of the features of polar codes application in 5G NR is presented in [23]. Using BLER and false-alarm-rate (FAR) characteristics, the corrective ability was evaluated and the computational complexity of polar codes was compared with LDPC codes. Belhadj and Abdelmounaim [24] examined the error correction performance of polar and LDPC code coding schemes when transmitting short and medium information blocks by employing BLER and BER metrics. Khan *et al*. [25] investigated LDPC and polar codes in terms of the frame error rate (FER) parameter, which is essentially the same as BLER, when transmitting short and medium length messages, considered multiple decoding implementation schemes and compared the error correction performance over the channel with AWGN.

In many of the works listed above, the study of the application of certain codes was carried out in the conditions of the AWGN channel only, without taking into account multipath effects. In numerous publications, the efficiency of codes application was made through the parameter of BER, in comparison with which such a parameter, as BLER, can have more value, because bits on the receiving side are also decoded by blocks. The research presented in this paper, particularly the calculation and selection of the basic parameters of the PDSCH signal and the size of the transmitted blocks, was conducted with reference to the realized 5G NR networks, although with a number of assumptions. Another important difference of this work is that the evaluation of the efficiency of polar and LDPC codes was carried out with the application of all standardized interleaving operations and CRC addition, performed at the level of the transmission line connection on the example of a PDSCH signal. In this study, the TDL and CDL multipath propagation models recommended by 3$^{\text{rd}}$ generation partnership project (3GPP) in technical report (TR) 38.901 [26] were applied to account for the effects of fading in the transmission channel, in addition to AWGN.

The remainder of this paper is structured as follows. Section 2 presents a brief description of LDPC and polar codes and the coding schemes used in 5G NR channels. Section 3 describes the metrics used to evaluate the coding efficiency. Section 4 is devoted to the description of the 5G NR propagation channel models. The methodology of the study and the calculations of the parameters required to perform the modeling are presented in detail in section 5, while section 6 presents the main results of the study. A discussion of the results and concluding comments are formulated in section 7.

2. CODING SCHEMES APPLIED IN 5G NR

The data link layer of 5G NR 3GPP standards includes the use of LDPC codes for downlink shared channel (DL-SCH) and uplink shared channel (UL-SCH), which have corresponding physical layers of physical downlink shared channel (PDSCH) and physical uplink shared channel (PUSCH). Polar codes are used in physical downlink control channel (PDCCH) and physical uplink control channel (PUCCH), where information blocks are small [2].

In our research for the projection of the experiment, we left our choice on the channel PDSCH. It is used to transport user data, paging messages, and responses to network access requests to all connected devices within the service area. PDSCH provides the physical layer for transporting DL-SCH and paging channel (PCH) channels, carrying information from higher layers. The modulation techniques (for physical

channels) and coding technologies (for transport channels and control information) used in 5G NR are summarized in Table 1.

Table 1. Modulation techniques and channel coding used in downlink and uplink

Transport channel/ control information	Supported channel coding	Appropriated physical channel	Supported modulation types
Downlink			
DL-SCH	LDPC	PDSCH	QPSK, 16-QAM, 64-QAM, 256-QAM, 1024-QAM
BCH	Polar code	PBCH	QPSK
PCH	LDPC	PDSCH	QPSK, 16-QAM, 64-QAM, 256-QAM, 1024-QAM
DCI	Polar code	PDCCH	QPSK
Uplink			
DL-SCH	LDPC	PDSCH	QPSK, 16-QAM, 64-QAM, 256-QAM, 1024-QAM
BCH	Polar code	PBCH	QPSK
PCH	LDPC	PDSCH	QPSK, 16-QAM, 64-QAM, 256-QAM, 1024-QAM
UCI	No coding is performed	PUSCH	PUSCH: $\pi/2$-BPSK, QPSK, 16-QAM, 64-QAM, 256-QAM
	Block code (for short message lengths)	PUCCH	PUCCH: $\pi/2$-BPSK, BPSK, QPSK

2.1. LDPC codes

LDPC codes were first presented by Gallager [27], but they were not used in their time and were forgotten for almost 40 years. Due to the advancement of computer technologies and new communications facilities, LDPC codes have become widely used for forward error correction (FEC) codes because of their superior error correction features and high parallelism in decoding implementation. Recently, LDPC codes have been used in many modern telecommunication technologies, such as DVB-S2, DVB-T2, DVB-C2, IEEE 802.3an, IEEE 802.11n and IEEE 802.16e. LDPC codes demonstrate high efficiency in terms of bit error probability, which is very close to the Shannon limit (0.6-0.8 dB loss for longer message lengths).

LDPC codes are linear block codes *(N, K)* defined by means of parity check matrix (PCM) *H* characterized by relatively small number of '1' in rows and columns. Sparsity of '1' provides low complexity of coding and decoding. An example of the matrix *H* (2, 4) (2 is the number of '1' (*j*) in each column, 4 is the number of '1' (*k*) in each row) of a regular LDPC code is given:

$$H = \begin{bmatrix} 0 & 0 & 1 & 1 & 0 & 0 & 0 & 1 & 0 & 1 & 0 & 0 \\ 1 & 0 & 0 & 0 & 1 & 0 & 0 & 0 & 1 & 0 & 1 & 0 \\ 0 & 1 & 0 & 0 & 0 & 1 & 1 & 0 & 0 & 0 & 1 & 0 \\ 0 & 0 & 1 & 0 & 1 & 0 & 1 & 0 & 0 & 0 & 0 & 1 \\ 1 & 0 & 0 & 0 & 0 & 1 & 0 & 1 & 0 & 0 & 0 & 1 \\ 0 & 1 & 0 & 1 & 0 & 0 & 0 & 0 & 1 & 1 & 0 & 0 \end{bmatrix} \tag{1}$$

It is often convenient to represent LDPC codes using a bipartite graph or Tanner graph [28]. It contains two types of nodes: check nodes (CN) corresponding to the rows of the matrix *H*, and variable nodes (VN) or bit nodes corresponding to the columns of *H* and bits of the codeword. Check node *j* is connected to variable node *i* if and only if the element h_{ij} in *H* is equal to '1'. For example, the Tanner graph of the matrix *H* is shown in Figure 1.
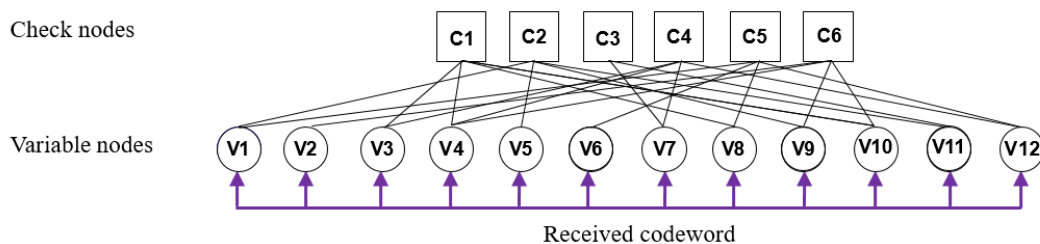

Figure 1. Representation of the parity check matrix H as a tanner graph

Among LDPC codes there are regular and irregular codes. The verification matrix of the former is characterized by the fact that all columns and rows contain the same number of '1' j and k, respectively. In irregular LDPC codes this property is not observed. For irregular LDPC code, we can say that the average number of '1' in a row and the average number of '1' in a column are small compared to the number of columns and the number of rows. Compared to regular LDPC, irregular LDPC has more design flexibility and optimization possibilities. 5G NR, like many telecommunication standards (IEEE 802.16, IEEE 802.11, and DVB-S2), utilizes a form of irregular LDPC codes such as quasi-cyclic LDPC (QC-LDPC) [29]. The following technical advantages of QC-LDPC can be noted: i) Relatively low error rate, suitable for systems with high reliability; ii) Decoding is highly parallelized, which ensures fast decoding and high data throughput; iii) QC-LDPC codes are relatively flexible and can be constructed with multiple code rates, numerous of block lengths, and several block sizes [30]. These are important in the construction of modern mobile and wireless communication systems; and iv) The decoding complexity decreases as the coding rate increases, which satisfies the requirement of high peak data rate.

The decoding process of LDPC codes is based on an iterative scheme between bit nodes and control nodes in a Tanner graph. The decoding scheme for LDPC codes is known as message passing algorithm (MPA), which iteratively passes messages back and forth between bit nodes and control nodes until a result is achieved (or the process is stopped). There are two basic approaches for decoding LDPC codes: decoding with "hard" (bit-flipping algorithm) and "soft" decisions (sum-product, min-sum algorithms). Decoders with soft decisions are more efficient, because they receive more information, but at the same time, they are more difficult to implement.

The bit-flipping algorithm is a MPA with hard decisions for LDPC codes [31]–[33]. Each received bit is processed by the detector, which makes a binary decision and transmits it to the decoder. For the bit-flipping algorithm, the messages transmitted along the edges of the Tanner graph are binary: a variable node sends a message declaring whether it is a one or a zero. Next, each check node performs a parity check on its associated variable nodes and then sends a message to each bit-flipping node associated with it, declaring what value the bit has based on the information available to that check node. If one (or more) variable nodes fail the parity check the greatest number of times, those nodes change (flip) their current values. This process is repeated until all parity check equations are satisfied, or until the maximum number of iterations has been performed.

Although bit-flipping algorithm is easy to implement, it is not as efficient as other algorithms, like the sum-product algorithm. This algorithm, also often referred to as the belief propagation (BP) algorithm, is MPA with soft solutions [34]–[38]. It is similar to the bit-flipping algorithm, but the difference is that the messages representing each decision are now probabilistic rather than discrete (or binary: '0' and '1'). While bit-flipping decoding makes an initial hard decision on the received bits as input data, the sum-product algorithm is a soft decision algorithm that takes the probability of each received bit as input data. The probabilities of the received input bits are called a priori probabilities, and the bit probabilities returned by the decoder are called posterior probabilities. In the case of sum-product decoding algorithm, these probabilities are expressed through log likelihood ratios (LLR) [38].

$$LLR = \ln \frac{\Pr(x=+1)}{\Pr(x=-1)} = \ln \frac{1-p}{p} \tag{2}$$

The advantage of the logarithmic representation of the probabilities is that, in case it is necessary to multiply the probabilities, it will be sufficient to add the LLRs, which will reduce the complexity of the decoder implementation. In BP algorithm, iteratively transmitted messages between nodes represent the belief level of the accepted codewords. Each variable node transmits a message to each control node connected to it. Each control node transmits a message to each bit node connected to that node. The goal of this algorithm is to compute the maximum a posteriori probability (MAP) for each bit of the codeword $P\{c_i = 1 \mid N\}$, which is the probability that the i-th bit of the codeword is equal to one provided that all parity check constraints are satisfied in event N. The final value of the decoded bit i is determined by comparing the sum of the LLR of this bit with the threshold value (zero).

The sum-product algorithm [39], which uses a probabilistic approach to decoding problems, has a better corrective ability compared to bit-flipping. However, at its use the computational costs increase, caused by necessity to use complex functions of hyperbolic tangent $tanh$ and arctangent $tanh^{-1}$ to form messages from check nodes to bit-flipping nodes. Therefore, for hardware implementation, the min-sum decoding algorithm, which uses an approximate computation of the check messages to the bit nodes, is widely used. Thus, instead of computing the product of the $tanh$ and $tanh^{-1}$, $sign$ and min operations are used, because of which the decoder is simpler in implementation and faster in processing time. In addition, there is no need to measure the noise variance value σ^2, which in the sum-product algorithm is included in

the LLR calculation formula as a scaling factor. For these advantages, the min-sum decoding algorithm turned out to be more preferable in practical implementations.

The number of computational operations per iteration for the sum-product algorithm compared to the bit-flipping and min-sum algorithms are approximately 8 and 3 times greater, respectively. At the same time, due to the simplification of calculations, the efficiency of the min-sum algorithm relative to the sum-product algorithm is reduced by about 0.2-0.5 dB. However, this loss can be reduced by some modifications of the min-sum algorithm, such as the min-sum normalized and min-sum offset algorithm [39]–[41]. It should be noted that the 3GPP technical specification (TS) 38.212 [2] does not impose strict requirements for the use of a particular LDPC decoding algorithm in any of the channels, leaving it to the discretion of the system designer. In this paper, we decided to focus on the BP algorithm as the most developed and widely used.

2.2. LDPC codes in 5G NR

As already mentioned, quasi-cyclic low-density parity-check (QC-LDPC) codes have been selected for use in 5G NR. The LDPC coding chain is shown in Figure 2 and includes code block segmentation, addition of CRC code, LDPC encoding, rate matching and systematic bit interleaving [2]. By segmenting code blocks, large transport blocks can be divided into multiple smaller blocks that can be processed efficiently in parallel by the LDPC encoder/decoder.

Figure 2. LDPC coding chain in 5G NR

The transport block is modified by adding CRC bits, the same way for downlink and uplink lines with their corresponding DL-SCH and UL-SCH channels. If the transport block size (TBS) corresponding to the sequence of information symbols *A* exceeds 3824 bits, a 24-bit CRC formed by the following generating polynomial is added to the end of the transport block: $g_{24A}(D) = [D^{24} + D^{23} + D^{18} + D^{17} + D^{14} + D^{11} + D^{10} + D^7 + D^6 + D^5 + D^4 + D^3 + D + 1]$. In other cases, a 16-bit CRC based on a generating polynomial $g_{CRC16}(D) = [D^{16} + D^{12} + D^5 + 1]$ is added to the end of the transport block.

Two base graph (BG) matrices, namely BG1 and BG2 [5], [42], were introduced in the TS 38.212 [2] to maintain scalability and compatibility of the data rate. When the TBS exceeds a threshold value (for BG 1 the threshold is 8,448 bits, for BG 2 the threshold is 3,840), the transport block undergoes segmentation by splitting into several code blocks of the same size. At the end of each code block, an additional 24-bit CRC is added after segmentation, obtained using the generating polynomial $g_{24B}(D) = [D^{24} + D^{23} + D^6 + D^5 + D + 1]$.

Rate matching performed by the circular buffer consists of adjusting the codeword length (*i.e.*, the number of coded bits at the output of the circular buffer) according to the available radio resources of the channel. In 5G NR LDPC, a row and column interleaver is used to interleave each code block after the rate matcher. The purpose of interleaving is to protect against packet interference. After interleaving, the original locally concentrated interference is distributed into separate isolated interference. Subsequently, small errors occurring during decoding are easier to detect and correct. The interleaver improves performance by making systematic bits more reliable than parity bits for initial code block transmission. Data is reordered based on the principle of line-by-line writing and column-by-column reading.

2.3. Polar codes

The basic idea of polar codes, first introduced by Arikan in [43], underlying the encoding and decoding algorithms of polar codes is channel polarization. Channel polarization is the operation of transforming a communication channel into *N* independent copies of it (virtual channels are created between input and output bits), in which the probability of error during data transmission tends to '0', or to '1' as the length of the information sequence increases. Information bits are transmitted through virtual channels having low error probability with high throughput, asymptotically reaching the Shannon limit. Thus, it becomes possible to efficiently utilize the communication channel and transmit messages through multiple channels possessing low error probability. Channels with error probability of '1' are called frozen, and no transmission is performed over them.

The concept of polar code formation is based on the Arikan kernel F_2. The Arikan kernel is a matrix, $F_2 = \begin{bmatrix} 1 & 0 \\ 1 & 1 \end{bmatrix}$ and through the value $F_N = F_2^{\otimes n}$ denote its n-th Kronecker degree [43]. The sequence needs to be transformed so that the number of the new position of the i-th element becomes the inverse of i, which is called polar representation, to obtain the required output vector. For example, $1 \equiv (0\ 0\ 0\ 1) \rightarrow (1\ 0\ 0\ 0) \equiv 8$. Thus, the permutation matrix B_N must be introduced to obtain the corresponding matrix. The resulting generating matrix G_N is defined by the following expression $G_N = B_N * F_2^{\otimes n}$. To perform the polarization operation, it is necessary to perform a transformation of the scalar channel into a vector channel, identifying it with the conditional probability density function of the output symbol [43], [44]. This is achieved by creating N-copies of the binary symmetric channel in a recursive manner, as presented in Figure 3.
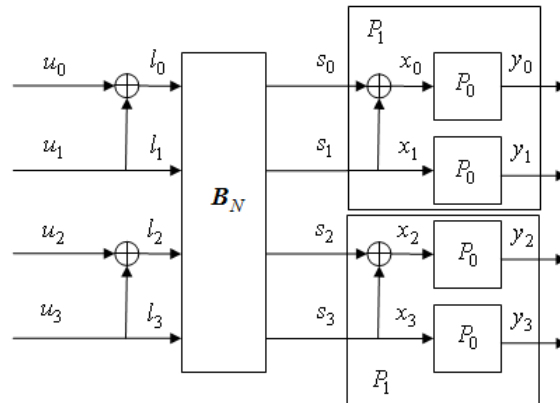

Figure 3. Recursive method of code vector formation

The idea of the traditional decoding algorithm for polar codes consists in sequential estimation of information bits. Such decoding algorithm is known as the successive cancellation (SC) algorithm [43]. The disadvantage of this algorithm consists that if on some step of decoding there is an error, then the estimation of all other bits also will be erroneous. Besides, application of SC algorithm leads to big decoding delays. For a codeword of length N, the total decoding delay of SC algorithm is equal to $(2N - 2)$ clock cycles, is a serious problem for application of polar codes in real-time applications.

Computational complexity (execution time) for encoding and decoding operations of polar codes by SC algorithm can be expressed as $O(NlogN)$, where N is the length of information sequence, the amount of memory required is $O(N)$. SC decoded polar codes have worse error correction performance at finite code length compared to modern channel codes such as LDPC and turbo codes. To improve the performance of polar codes, improved versions of the SC algorithm, such as successive cancellation list (SCL) and successive cancellation stack (SCS), have been developed, which perform much better than the SC decoding algorithm, although they have higher complexity compared to SC. Furthermore, CRC codes are combined with polar codes that are decoded using the SCL algorithm. The performance of a concatenated system outperforms other cutting-edge channel codes.

One of ways to overcome dependence on estimates of preceding bits at decoding of polar code is to use of SCL algorithm Tala-Vardi [45]. It allows to increase efficiency of decoding of polar code at transmission of small and medium size messages. In this algorithm for decoding of input bits one by one L best decoding paths are simultaneously tracked, unlike SC decoding method, in which only one path is tracked. This algorithm allows to realize decoding comparable to the maximum likelihood method already for a small list size ($L = 16$). The complexity of the SCL algorithm depends on the size of the list. Its time complexity is equal to $O(LNlogN)$, and its memory complexity is equal to $O(LN)$.

An improved version of the SC algorithm called successive cancellation stack (SCS) is proposed in [46]. It uses a stack for storage and determines the best candidate path by optimal search. Whenever the best path reaches a metric value, the decoding operation is stopped and a decision is made about the bits transmitted. The length of the candidate paths is what distinguishes SCL from SCS. Candidate paths in the SCL algorithm have the same length, but in the SCS algorithm, they can vary in length. The largest stack value in the SCS decoder is D, and the number of expanding paths is limited by L. Then the computational and memory complexity for SCS is defined as $O(LNlogN)$ and $O(DN)$ respectively. The parameter L is

usually taken small of the order of '8', *D* should be of the order of the code length *N*. Note that the recommendation TS 38.212 [2] suggests using in channels with polar coding exactly decoding algorithm CRC-aided SCL (CA-SCL), so in our work we applied it.

2.4. CRC-aided polar codes in 5G NR

Uplink and downlink control information (UCI and DCI) is being encoded using polar codes as the coding scheme for 5G NR [1]. DCI involves concatenating polar codes with distributed CRC, which bits are derived by interleaving bits between the CRC encoder and the polar encoder. Thus, 5G new radio uses a CRC-aided polar coding scheme (CA-Polar). The interleaving distributes the CRC bits in such a way that the CRC bit is positioned by the last bit needed to compute it [47]. Therefore, decoding complexity can be reduced by stopping decoding early when an incorrect check is detected [48], [49].

The implicit CRC encoding of downlink (DCI or BCH) or Uplink (UCI) message bits dictates the use of CRC-aided serial cancel list (CA-SCL) decoding [50] as a decoding algorithm. CA-SCL decoding has been known to outperform LDPC or turbo codes [51], leading 3GPP to adopt polar codes. CA-SCL decoding will exclude paths that have invalid CRCs when an input message is combined with one, as long as at least one path has a valid CRC. The CA-SCL decoder performs better when this operation is used in the final path selection than when it is used in SCL decoding. A CRC of 24 bits is used for the downlink, while CRCs of 6 and 11 bits are specified for the uplink, which vary depending on the value of the transmitted information block length. The Figures 4(a) and 4(b) show the coding chains of 5G NR polar codes for uplink and downlink [2]. Some of the listed operations are performed only in the uplink or downlink. The main components of the coding chains are CRC encoder, polar coding and rate matching.
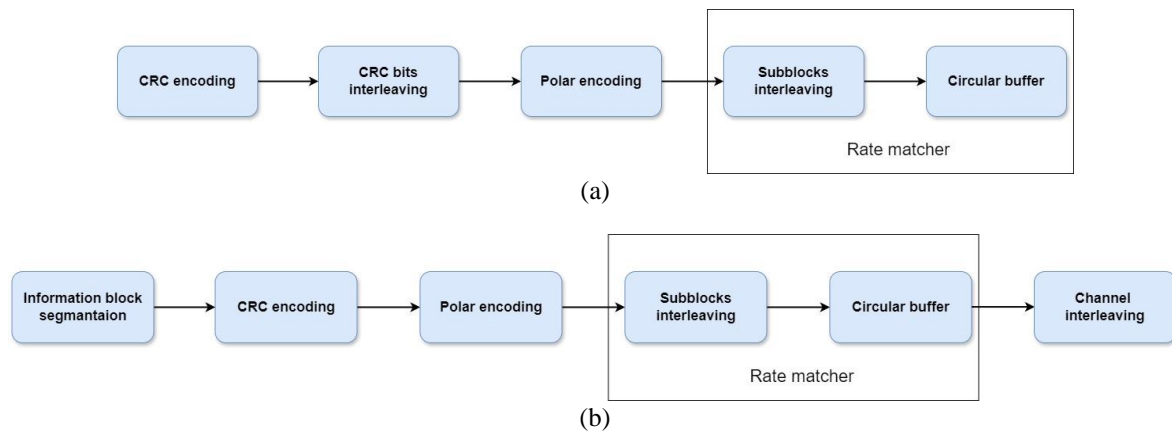

(a)

(b)

Figure 4. Polar code encoding chain in 5G NR for (a) downlink and (b) uplink

Segmentation involves dividing the original information block into several subblocks before performing polar coding for each subblock. Segmentation is only performed in Uplink during UCI signaling and is only required when the information block size exceeds a certain length and sufficient radio resources have been allocated. The CRC parity bits are used for error correction at the end of SCL decoding to eliminate decoding paths in the list that do not match the CRC and to select the most probable codeword. After that, the information sequence is polarized for a given size code $N = 2^n$.

For all information block lengths in the PDCCH and PBCH channels, a 24-bit CRC is used, which is obtained using a generating polynomial $g_{\text{CRC24C}}(D) = [D^{24} + D^{23} + D^{21} + D^{20} + D^{17} + D^{15} + D^{13} + D^{12} + D^8 + D^4 + D^2 + D + 1]$. In the case of a PUCCH channel with information block length $A \in [12, 19]$, a 6-bit CRC is used, which is obtained using a generating polynomial $g_{\text{CRC6}}(D) = [D^6 + D^5 + 1]$. If the information block size $A \in [20, 1706]$ in the PUCCH channel, then the following is used 11-bit CRC formed by a generating polynomial $g_{\text{CRC11}}(D) = [D^{11} + D^{10} + D^9 + D^5 + 1]$.

CRC bit interleaving is a component of the coding chain that is performed only in downlink. The purpose of the CRC interleaver is to distribute the CRC bits within a block more evenly among the informational and frozen bits. To calculate the value of a CRC bit, it is necessary to wait for the information bits that come after a given CRC bit, as the CRC interleaver is designed to depend solely on the previous information bits during SC/SCL decoding. Distributed CRC bits make it possible to conduct CRC checks earlier in the decoding process and stop the list decoding process when all candidate paths fail CRC checks.

Rate matcher, which consists of a subblock interleaver and a circular buffer, is tasked with adjusting the codeword length in accordance with the available radio resources of the channel. Before being inserted into the circular buffer, the subblock interleaver aims to group the coded bits in the order they are discarded or received. Concatenating the bits of each encoded block is done after the rate matcher, and the output data is sent for further processing. Afterward, the coded bits are dedicated to be transmitted by the rate matcher, and all coded blocks are merged together. The output bits are sent for more processing. Channel interleaver is implemented to reduce the negative effects of fading in the propagation channel and reliability differences between individual bits of the UCI signal on transmission efficiency. A triangular interleaver is used for 5G NR polar codes with a line-by-line decrease in column count per row. When using high order modulation, the efficiency of the polar NR code can be greatly improved by this interleaver.

3. CODING PERFORMANCE METRICS
3.1. Reliability

BER and BLER are most commonly used to evaluate the reliability of message transmission in digital communication systems. Both are important for understanding the overall performance of a communication system. BLER indicates the quality of the entire transmission channel, while BER can only reflect an estimate of the coding efficiency. Therefore, BLER is the parameter that must be achieved in order to provide a particular service.

BER is the ratio of the number of bits erroneously received by the receiver to the total number of bits transmitted by the transmitter. BER can be divided into two types depending on how it is measured. The first is transport BER, which is the ratio of detected incorrect bits before error correction to the total number of bits transmitted (including redundant code bits). The second option is the information BER, which is the number of decoded bits remaining incorrect after error correction divided by the total number of decoded bits (useful information). It is often the second variant that is used.

The BLER parameter, in some cases also defined as frame error rate (FER), is defined as the ratio of the number of erroneous blocks received Blk_{err} to the total number of blocks sent Blk_{transm}:

$$BLER = \frac{Blk_{err}}{Blk_{transm}} \tag{3}$$

A single bit error in the entire frame is considered a frame error; typically, the frame is discarded and a retransmission is requested. An erroneous block is defined as a transport block whose CRC check is incorrect. At the link layer, the system can work only with whole message frames, not with individual bits. In this case, if a transmission error occurs, the data can be restored to the original state due to the efficiency of the decoding algorithm.

An alternative parameter for assessing the effectiveness of the application of an interference-resistant code can be the relative channel capacity, which is defined as the ratio of the number of successfully transmitted transport blocks Blk_{suc} to the total number of transmitted blocks Blk_{all}. Being, in fact, another representation of BLER. It allows to observe actually available in these conditions the resource of the radio line, and, if necessary, to be reduced to absolute values of the transmission rate.

$$Thrput = \frac{Blk_{suc}}{Blk_{all}} = 1 - BLER \tag{4}$$

3.2. Delay

The total service delivery delay of a 5G communication system is defined as radio interface delay, processing delay, and transmission delay within and outside the 5G system. End-to-end delay is the required time from the time the target information is transmitted by the source to the time the information is fully received by the destination, which includes transmission delay, queuing delay, computation delay, and retransmission delay. The impact of delay should always be considered in code design. Without delay limitation, arbitrary reliability can be achieved by retransmission or code rate reduction. The total end-to-end delay T_{total} can be expressed as (5):

$$T_{total} = T_{dec} + T_{transm_{enc}} + T_{transm_{dec}} + T_{prop} + T_{mod} + T_{dem} \tag{5}$$

where T_{dec} is the decoding delay, $T_{transm\,enc}$ and $T_{transm\,dec}$ are the block transmission time in the encoder and decoder, T_{mod} and T_{dem} are the modulation and demodulation delays, and T_{prop} is the propagation delay.

At a given bit rate, the block transmission time in the encoder and decoder can be considered the same, that is, the buffer fill time. On the other hand, the decoding time is limited from above by the block

transmission time to prevent buffer overflow. Let T_{transm} represent the block transmission time, and then the expression (5) can be rewritten as:

$$T_{total} \geq T_{dec} + 3T_{transm} + T_{prop} + T_{mod} + T_{dem} \tag{6}$$

3.3. Computational complexity

Computational complexity is also a very important parameter of decoding. Without limitation of computational complexity, maximum likelihood (ML) decoding method will always be optimal in terms of reliability for any codes. Hence, the goal of designing a decoding scheme is to achieve decoding performance close to ML with a reasonable level of complexity. Decoding complexity is an important delay factor, since the decoding time is one of the main parts of the total end-to-end delay.

a. LDPC codes: belief-propagation decoding algorithm

In the BP algorithm, the decoding complexity is composed of the number of addition operations and reference table access operations [52]. For hardware implementation, table access operations are desirable because they can be accomplished with a small amount of memory in the form of an array indexing operation. Memory reads can take less processing time than conventional operations such as multiplication, addition, and so forth. The complexity of adding and accessing the table while decoding can be estimated using expressions (7) and (8) respectively:

$$I_{max} \times O\big(2 \times N \times d_v + M \times (2 \times d_c - 1)\big) \tag{7}$$

$$I_{max} * O(M \times d_c) \tag{8}$$

where I_{max} is the maximum number of decoding iterations, N is length of LDPC code, d_v is average value of the variable node in the PCM, M is number of parity check bits, d_c is average value of check node in the PCM.

b. Polar codes: successive cancellation list algorithm

In the case of the SCL decoding algorithm [53]. Its complexity is estimated as (9):

$$O(L * N * log_2 N) \tag{9}$$

where L is the depth of the successive cancellation decoding list, N is polar code length.

4. PROPAGATION CHANNEL MODELS USED IN 5G NR

Before designing, modeling and planning wireless systems, it is necessary to set the parameters of a channel propagation model. They can provide information about the future structure, performance, efficiency, and accuracy. Most of the above-mentioned works on channel modelling in 5G NR used the following models, for which we give a brief comparison below.

4.1. Stochastic Rayleigh and rice channel models

Stochastic channel models simulate the probability density function (PDF) of the channel impulse response (or equivalent functions). Instead of accurately predicting the impulse response at a single location, these methods aim to predict the PDF across a large area. Using stochastic models is more common for system design and comparison.

A channel with Rayleigh fading occurs when there are many different signal paths between the transmitter and receiver, none of which is dominant (the case of NLOS). The model describes a worst-case scenario in the sense that the dominant component of the signal is missing and therefore there are many dips with fades. This assumption is useful for the design of reliable systems. The Rayleigh PDF of the envelope of the received signal $p(r_0)$ is written as (10):

$$p(r_0) = \frac{r_0}{\sigma^2} \exp\left(-\frac{r_0^2}{2\sigma^2}\right); \; r_0 \geq 0 \tag{10}$$

where σ^2- average power of the multipath signal.

The rice fading channel model is used when the received signal is a combination of a significant line-of-sight (LOS) path and several fading paths between the transmitter and receiver. Due to LOS, the effect of Rayleigh fading on the transmitted signal will be less than in the case of Rayleigh fading. The Rice probability density function of the envelope of the received signal is defined by the expression:

$$p(r_0) = \frac{r_0}{\sigma^2} \exp\left[-\frac{(r_0^2+A^2)}{2\sigma^2}\right] I_0\left(\frac{r_0 A}{\sigma^2}\right); r_0 \geq 0, A \geq 0 \qquad (11)$$

where $I_0( )$ is the modified zero-order Bessel function and A is the peak magnitude of the LOS signal component.

In the rice channel with fading, the K-factor is one of the input parameters determining the power ratio of the LOS component to the multipath component ($K = A^2/2\sigma^2$). The stronger the LOS component, the less frequently deep fading occurs. When K is zero, the channel with Rice fades becomes a channel with Rayleigh fades. When K increases, the Rice channel approaches a Gaussian distribution with mean A.

4.2. The channel models proposed by 3GPP

In the 3GPP technical report (TR) 38.901 [26], two propagation channel models, clustered delay line (CDL) and tapped delay line (TDL), were presented. In both models, multipath propagation parameters such as power and receive delay of the signal are taken into account. The CDL models also take into account the scattering in the angles of arrival and departure in spherical coordinates in azimuth and elevation, which are used in comparing antennas with different patterns.

A feature of TDL/CDL models, in contrast to the geometric model of the radio channel, is the approach to determining the signal power. Instead of exact calculation of the incoming signal power from individual antennas and individual time reports, the power is described by some random distribution (Rice or Rayleigh) with respect to some average value of the received power. Thus, the mean value is the input parameter of these models, given by the value of the signal-to-interference-plus-noise ratio (SINR). Within each of these models, there are profile variants that simulate both the absence of line of sight (models CDL-A, CDL-B, CDL-C and TDL-A, TDL-B, TDL-C) and its presence (CDL-D, CDL-E and TDL-D, TDL-E), and have different values of propagation delay and signal attenuation from each other.

TDL model is intended for simplified calculations, such as the single input single output (SISO) situation. The paths between transmitter and receiver are characterized using statistical parameters, with no reference to the environment's geometry, using Rice and Rayleigh distributions. Each tap in the time domain has its own time-varying amplitude and delay coefficients. An illustration of the TDL channel model is shown in Figure 5.

CDL model represents a channel in which the received signal consists of a number of distinct delay clusters. Each cluster contains a number of multipath propagation components with the same delay value but with small differences in arrival and arrival angles. An example of the model for the case of two clusters is shown in Figure 6.
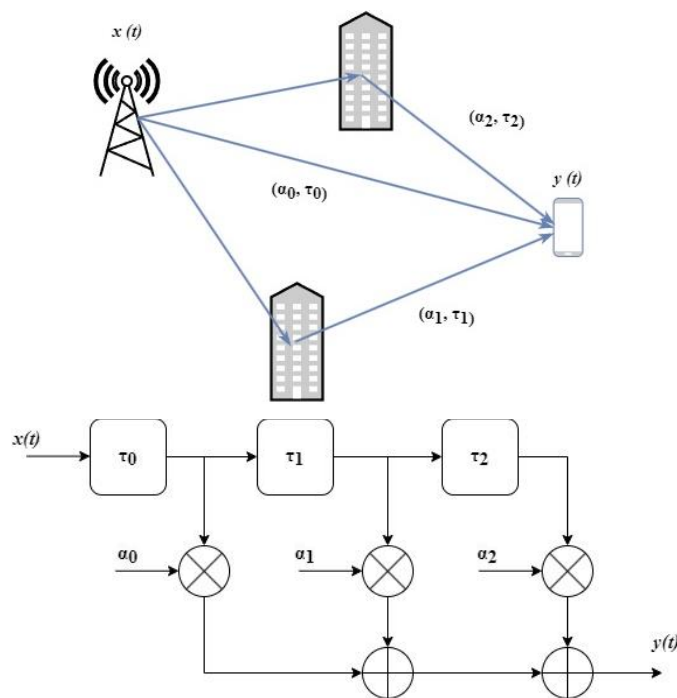

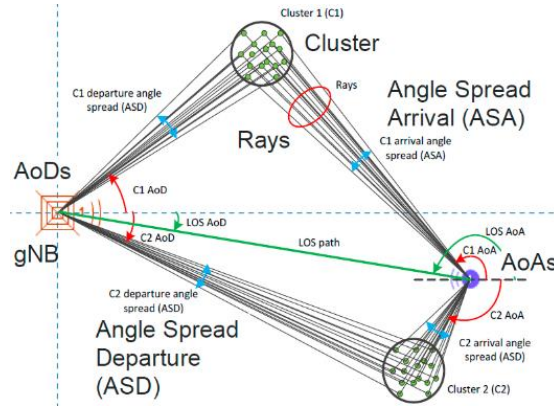Figure 5. Example of TDL model for the case of three branches

Figure 6. Example of CDL model for the case of two clusters

Other researchers have developed their own methods for calculating signal loss in multipath propagation channels, providing a wide range of considered application scenarios for studying 5G standard signals within their framework. For example, we can mention projects such as METIS, NYU WIRELESS, MiWEBA, and QuaDRiGa, which have been described in detail and compared with each other in [54]. However, since the application of these models was not planned for this paper, it was decided not to present them even briefly.

5. METHOD

Before the direct evaluation of the efficiency of the applied codes, it is necessary to determine the parameters of the radio signal. Preliminary assume that the modeling will consist PDSCH channel under multipath propagation conditions. Modulation schemes and coding rates of transport blocks sizes will be calculated below.

5.1. Observed transmission rates as a basis for the initial parameters

To determine the initial modeling parameters, we have decided to refer to the indicators recorded in the 5G networks launched as of July 2022 and presented in the document [55]. Having averaged the results of download speeds of ten leading operators in the category "5G download speed - global," the initial value of channel throughput of 380 Mbps was established. Later, with the release of a new report [56] illustrating performance at the time of 2023, the leader information was updated and a new bar for average peak speed of 404.4 Mbps was set. We have studied the data on the launched 5G networks presented in the reports [55], [56], and have taken into account the information from source [57]. Based on these, we chose signal parameters such as the frequency range (in our case, it is n78, which provides balance of coverage and throughput), and 100 MHz bandwidth.

5.2. Estimation of theoretical maximum throughput capacity

The maximum throughput is the highest value of throughput that can be achieved only under ideal conditions. The main reason for calculating this value is to obtain a rough estimate of the upper bound on the throughput that the system can provide. After determining the value of maximum RB allocation $N_{PRB}^{BW(j),\mu}$ from TS.38.104 [58], it is possible to compute the approximate maximum data rate with TS 38.306 by [59] utilizing the expression (12):

$$Data\ Rate\ (Mbps) = 10^{-6} \times \sum_{j=1}^{J}$$

$$\left(v_{Layers}^{(j)} \times Q_m^{(j)} \times f^{(j)} \times R_{max} \times \frac{N_{PRB}^{BW(j),\mu} \times 12}{T_s^{\mu}} \times \left(1 - OH^{(j)}\right) \right) \qquad (12)$$

where J is number of aggregated component carriers (CC); R_{max} is maximum code rate, $R_{max} = 948/1024$; μ is numerology index; T_s^{μ} is average OFDM symbol duration in a subframe ($T_s^{\mu} = \frac{10^{-3}}{14*2^{\mu}}$); $f^{(j)}$ is scaling factor; and $OH^{(j)}$ is overhead.

With an initial average throughput target of 380 Mbps (determined from the report [56]), we achieved a near target rate of 376.659 Mbps with 1 component carrier, 22 RB allocated to the user, 256-QAM modulation and 8×8 multiple-input multiple-output (MIMO) configuration. For further consideration, we defined three signal configurations: high, medium and low speed with 256-QAM, 16-QAM and quadrature phase shift keying (QPSK) modulations, respectively. Since this work does not consider the use of MIMO technology in the simulation of the Tx-Rx system, which corresponds to the situation of SISO, the parameter (number of layers) should be changed to '1' in further calculations. The other parameters are identical to those used in previous calculations. The parameter values and channel throughputs are presented in Table 2.

5.3. Calculating the transport block size

Since the transmission of data packets generated within encoders is considered, it is necessary to relate specific transport block sizes to the previously prepared configurations. At the physical layer, the amount of data to be transmitted is related to the transport block size (TBS). It is important to note that the TBS calculations using the methodology outlined in recommendation TS 38.214 [60] assume the use of LDPC code in the PDSCH channel. The transport block sizes, code rates and modulation orders for the polar code case are assumed to be equal to those obtained for LDPC, if no restrictions are encountered.

The concept of a resource block (RB) differs from a physical resource block (PRB), which follows, in that the former refers to the 5G NR signal over the entire carrier spectrum allocated by the operator for transmission. To aid in the power saving of mobile devices, only a portion of the carrier, called the bandwidth part, is accessible to them. One of the limitations to the application of polar codes in 5G NR is the relatively small limit size of the encoded block at the output of the encoder. In the case of downlink, the codeword length is 512 bits (according to TS 38.212 [2]), with a maximum of 140 bits of information symbols. Therefore, in order to implement using of polar encoder in the medium- and low-speed configurations, we have decided to change the number of allocated resource blocks and the number of allocated PDSCH symbols within the slot to fit the codeword boundaries. Table 3 shows the obtained TBS and the parameters used in their calculation.

Before the simulation, we also had to determine the minimum required value of the BLER probability. The TBS and modulation coding scheme (MCS) discussed above can be linked to the BLER via the channel quality indicator (CQI) parameter. It indicates the fastest modulation scheme and code rate that a user equipment (UE) can handle with a specific BLER value. Depending on the configuration, the mobile device can report CQI in three ways, which are described in [60]. Each of them corresponds to a specific use scenario (eMBB, mMTC, URLLC), the maximum modulation order and the permissible BLER value (10% or 0.001%). Since we have considered the eMBB scenario in our paper, we will set the BLER threshold of 10% for all previously specified configurations.

Table 2. Signal configurations and their parameters

Parameters	Values		
Duplex mode	TDD		
Frequency band	n78		
Numerology used	1		
Subcarrier spacing	30 kHz		
Maximum RB allocation $N_{PRB}^{BW(j),\mu}$	273		
OFDM symbol duration in a subframe	35.7 µs		
Overhead	0.14		
Number of aggregated CC	1		
Scaling factor $f^{(j)}$	1		
Number of layers $v_{Layers}^{(j)}$	1		
Configuration	High-speed	Medium-speed	Low-speed
Modulation order $Q_m^{(j)}$	8	4	2
Channel throughput, Mbps	47.082	23.54	11.77

Table 3. Signal configuration parameters before/after adjustments

Configuration	High-speed	Medium-speed	Low-speed
Codes used	LDPC	LDPC/Polar	LDPC/Polar
Modulation	256-QAM	16-QAM	QPSK
Code rate	948/1024	340/1024	251/1024
Number of allocated RBs	22	22/1	22/1
Number of PDSCH symbols within the slot	14	14/9	14/9
Number of DM-RS symbols in PRB	4	4	4
Number of signaling symbols	0	0	0
Transport block size (TBS)	25608	4480/136	1736/48

5.4. Multi-path propagation model selection

From the set of propagation channel models for 5G NR discussed above, we decide to focus on the CDL and TDL models for use in our work. TDL-A/CDL-A and TDL-D/CDL-D models (NLOS and LOS respectively) are compared to assess the impact of propagation model on signal transmission quality between base station (BS) and UE. We have chosen urban macro outdoor-to-outdoor (UMa O2O) signal propagation scenario, where the BS is installed above the roof levels of surrounding buildings [26]. Based on the values presented for a number of scenarios and signal frequencies, we determined the desired delay of the propagation of the signal in 100 ns. We also set the Doppler frequency of the UE at 12.963 Hz based on its speed of movement in 4 km/h and signal frequency of 3.5 GHz.

One of the components of the BS Tx-Rx system is an equalizer, which performs an evaluation of the transmission channel to further adjust the received signal to reduce the effects of inter-symbol interference (ISI) and noise to ensure recovery of the transmitted symbols. One widely used type of equalizer is the MMSE, which was implemented in our model. It minimizes the root mean square error between the transmitted signal and the corrected received signal by balancing ISI elimination with noise gain control.

6. RESULTS AND DISCUSSION

In the final part of this paper, we compared the effectiveness of PDSCH 5G NR Polar and LDPC polar encoding messaging using the CDL-D/CDL-A and TDL-D/T-A multipath propagation models. The simulation was performed in the MATLAB 2022b environment, which provides a range of options and customization for the signal components of the 5G NR standard, allowing for all necessary processing steps in the polar and LDPC encoding chains as specified in [2]. When simulating signal configurations for selected SNR values to evaluate transmission quality, we used a sequence of 20,000 information blocks. The values of SNR were preliminarily determined, above which BLER takes values significantly lower than the target value of 10%. We assumed that the ideal channel estimation is applied in the MMSE equalizer used. It is important to note that our system did not use block retransfer, unlike the 5G NR system, which uses hybrid automatic repeat request (HARQ). Figure 7 shows a block diagram of the model used and the main operations performed in it.

The performance of interference tolerant coding will be evaluated through the BLER and the absolute channel throughput. The values of SNR ratio were preliminarily determined, above which BLER takes values significantly lower than the target value of 10%. Table 4 lists the main parameters of previously prepared signal configurations. The simulation results are presented in Figures 8 to 12.

Figures 8(a) and 8(b) illustrate the comparison of the efficiency of LDPC coding application in high-speed configuration through the BLER. Thus, with a BLER of 10%, the CDL-D model (~28.9 dB) has a gain over the CDL-A model (~37.6 dB) of the order of 9 dB. In the case of the TDL models, achieving a BLER of 10% for TDL-D requires an SNR of about 26.4 dB, which gave a similar (to the CDL models) gain of 9.1 dB over the TDL-A model with 35.5 dB.

Figures 9(a) and 9(b) show the comparison of channel coding performance in medium-speed configuration. We can observe a significant gain of polar code over LDPC in both LOS situation (the target BLER under polar code and CDL-D model was achieved at SNR of ~3.5 dB vs 9.7 dB (6.2 dB) LDPC code) and NLOS situation (6.9 dB and 13.5 dB (6.6 dB), respectively). In the case of the TDL models, the polar code efficiency gains are similar (2.6 dB vs 7.9 dB (5.3 dB) for TDL-D and 6.5 dB vs 11.8 dB (5.3 dB) for TDL-A), but the gap of results between the LOS and NLOS models has narrowed compared to the CDL models.
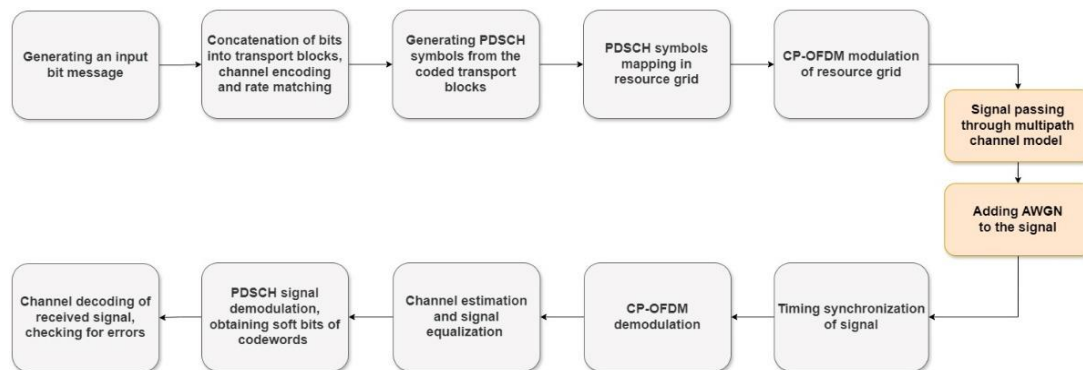

Figure 7. Block diagram of the simulation model

Table 4. Main parameters of previously prepared signal configurations

| Parameter	High-speed	Medium-speed		Low-speed	
Subcarrier spacing		30 kHz			
Cyclic Prefix		Normal			
Sample rate		3.84 MHz			
Transmission bandwidth	22 RB	1 RB		1 RB	
Modulation order	256-QAM	16-QAM		QPSK	
Number of PDSCH-symbols in slot	14	9		9	
Number of layers	1	1		1	
Channel encoder	LDPC	LDPC	Polar code	LDPC	Polar code
Channel decoding algorithm	BP	BP	CA-SCL	BP	CA-SCL
Coding rate	0.926	0.332		0.245	
Number of CRC bits	24	16	24	16	24
TBS before/after encoding	25608/27456	136	380	48	196
Channel delay spread		100 ns			
UE Doppler frequency		12.963 Hz			
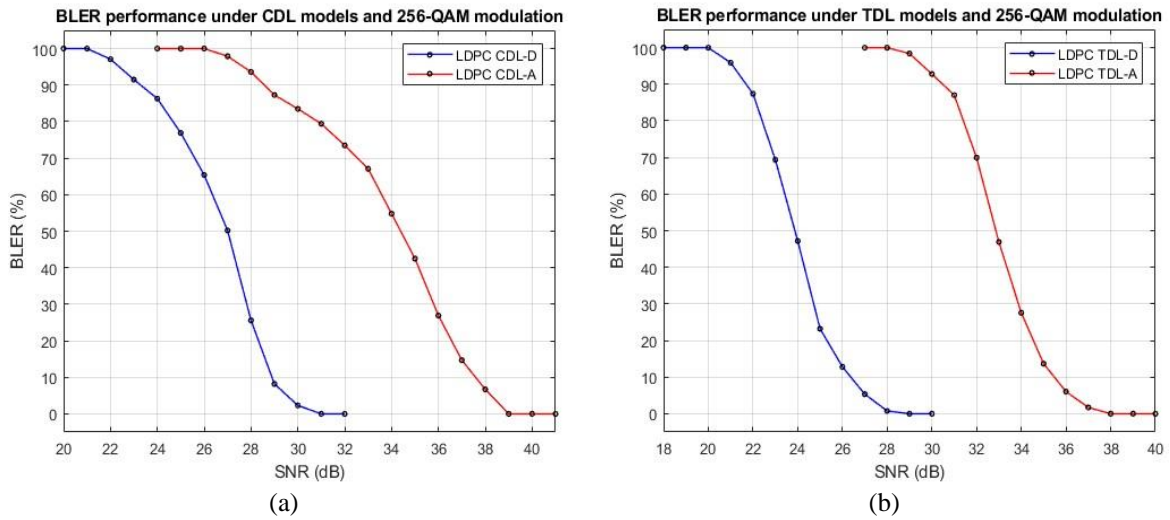
Figure 8. Performance comparison between CDL-D and CDL-A channels (a) TDL-D and TDL-A channels and (b) in the case of high-speed configuration
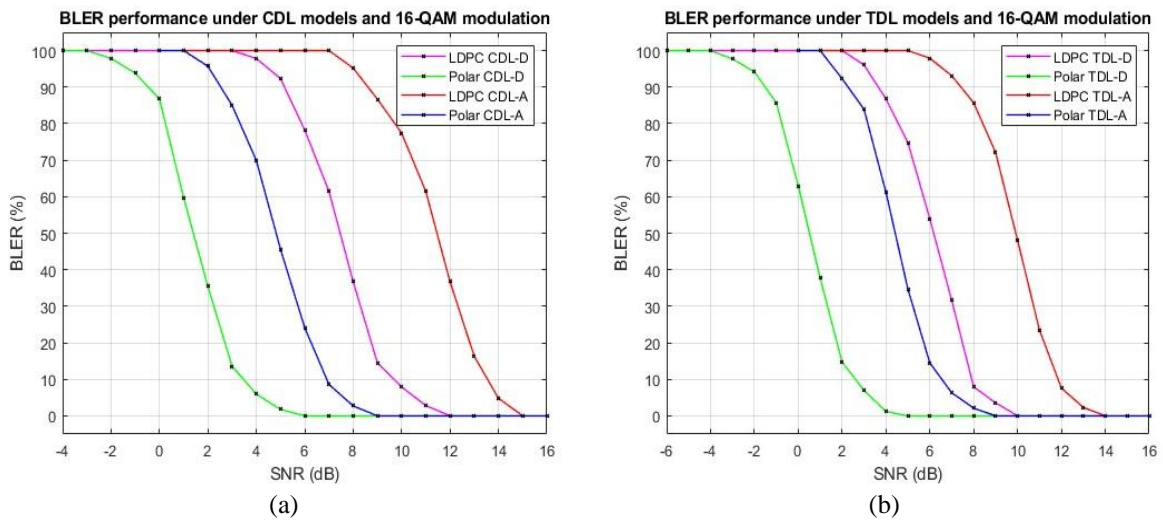

Figure 9. Performance comparison between CDL-D and CDL-A channels (a) TDL-D and TDL-A channels and (b) in the case of medium-speed configuration

Figures 10(a) and 10(b) display the comparison of channel coding performance in low-speed configuration. Similar to the previous results, the polar code shows coding gains over LDPC codes in all cases we investigated (0.8 vs 5.6 (4.8) for CDL-A, -1.8 dB vs 2.7 dB (4.5 dB) for CDL-D, 0.3 dB vs 4.5 dB (4.2 dB) for TDL-A, and -2.6 dB vs 1.5 dB (4.1 dB) for TDL-D), albeit slightly reduced. Thus, while for 16-QAM modulation the differences in gain were of the order of 6.2 dB and 5.3 dB (for the CDL and TDL models, respectively), in this case it was 4.6 dB and 4.1 dB.

For all simulation results, it is important to note that it was only possible to obtain them by applying equalization of the received signals by EQ due to the perfect estimation of the current channel state. Without this, correct decoding would not have been possible, as can be seen in Figures 11(a) and 11(b) for the example of medium-rate configuration signals. As an alternative to the BLER plots, we also considered the absolute throughput of the model. Thus, in Figures 12(a) and 12(b) we present the results obtained for a medium-speed configuration, similar to those shown in Figures 8(a) and 8(b).

Although the complexity and decoding latency of different coding technologies were not considered in this paper, however, on average, modeling the polar code case took about 2-2.5 times longer than the LDPC case. Thus, on our hardware (AMD Ryzen 5 4600H 3.00 GHz processor running Win 10) it took about 150 seconds to transmit 10000 slots in the LDPC case and 360 seconds in the polar coding case.
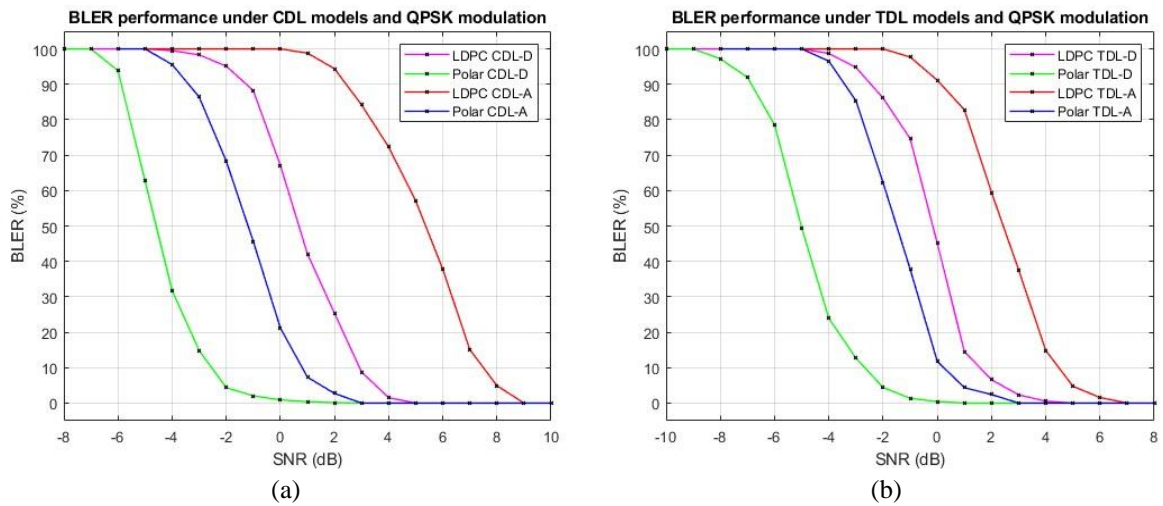

(a)   (b)

Figure 10. Performance comparison between CDL-D and CDL-A channels (a) TDL-D and TDL-A channels and (b) in the case of low-speed configuration

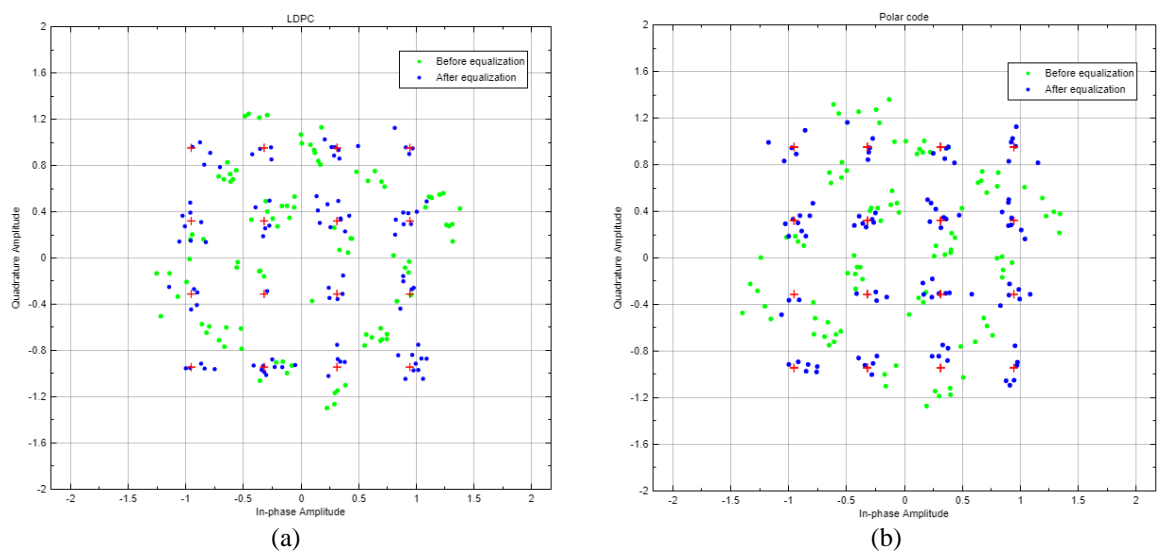(a)   (b)

Figure 11. Signal constellations of modulated signals using (a) LDPC and (b) polar coding. Red crosses represent reference constellation
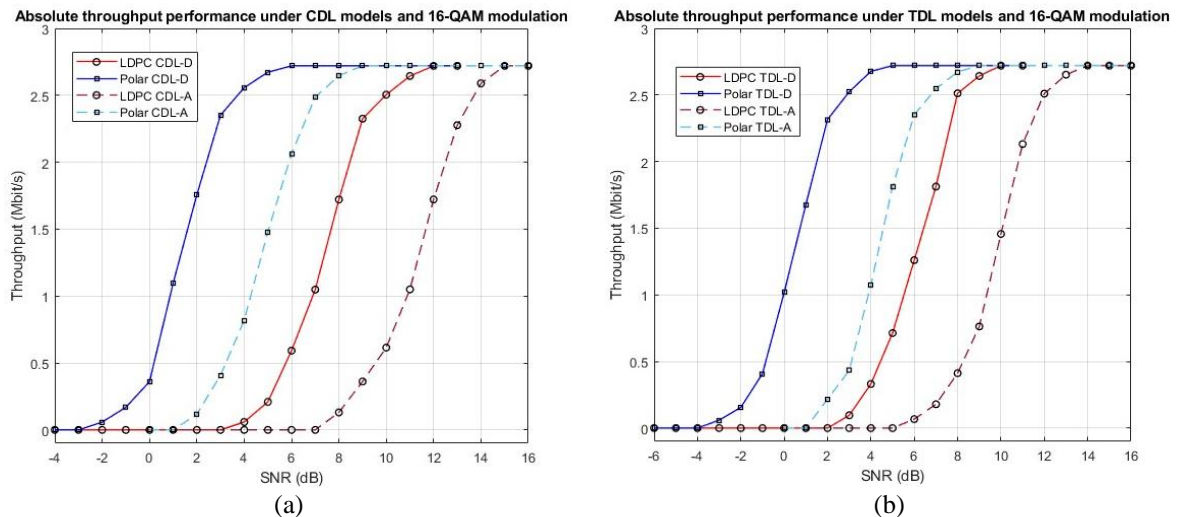
Figure 12. Comparison of absolute channel throughputs for the case of medium-speed configuration in (a) CDL-D/CDL-A and (b) TDL-D/TDL-A channels

Considering all the above results, the following can be noted:
− To achieve the target BLER of 10% for both LDPC and polar coding, the CDL channel models have more stringent SNR requirements than TDL models. Figures 8-10 show that as the codeword size and modulation order decreased, this difference decreased for the LOS and NLOS models.
− In the NLOS scenario, the target BLER values for each signal were achieved at significantly higher SNR than in the LOS case. For both types of models in each configuration, the differences in required SNR were compatible.
− The advantage of using polar codes over LDPC codes is noticeable. For the channel models with LOS (CDL-D and TDL-D) this difference was slightly larger than in the NLOS case (CDL-A and TDL-A).
− With decreasing modulation order and corresponding codeword size, the advantage of polar code over LDPC code decreased.

The correctness of our results is confirmed by comparison with related works [16], [17]. However, we should again note that in this study, such features of the realized networks as the used frequency range, spectrum bandwidth, and the transmission throughput recorded during measurements and a number of related parameters were taken into account when preparing the model.

7.   CONCLUSION

In this paper, we have conducted a detailed study of the efficiency of LDPC and polar coding techniques supported in 5G NR networks for several values of transmitted information block lengths in the PDSCH transmission channel. We studied the advantages and limitations of the application of the considered coding techniques in 5G systems, analyzed the data on the currently launched networks of mobile operators, which we took into account when selecting the initial parameters of the channel simulation model. Also, using the necessary documentation of the 3GPP consortium, we calculated the necessary parameters of the carrier signal of the PDSCH channel, which in the framework of our study was affected by multipath propagation using TDL and CDL channel models.

From the simulation results for the previously trained signal configurations, we observed a severe gain of polar codes over LDPC codes, which decreases as the codeword length decreases. We also note a significant increase in the required SNR to achieve the target BLER when moving from the LOS to NLOS situation in the TDL and CDL models. The results obtained can be useful in practice for the deployment of new 5G networks to determine the feasible radio range that maintains the target BLER performance. The developed model provides the reader with a convenient description to understand, implement and simulate 5G-compliant channel codes and radio signals.

Our focus for future research is to examine the performance of current channel codes in other multipath propagation channel models and other application scenarios for 5G systems, including using MIMO technology, which is possible with the model developed in this paper. In addition, as already noted, one of the main disadvantages of using polar codes in transmission channels is a large decoding delay.

Therefore, one of actual directions of continuation of researches in theoretical area is studying of possibilities of optimization of structure of polar coder and application of parallel calculations at its decoding, allowing to increase efficiency and speed of decoding that can promote further introduction of polar codes in perspective communication systems.

REFERENCES

[1] ITU, "Framework and overall objectives of the future development of IMT for 2020 and beyond," *International Telecommunication Union (ITU)*, 2015. Accessed: Jun. 14, 2024. [Online], Available: https://www.itu.int/dms_pubrec/itu-r/rec/m/r-rec-m.2083-0-201509-i!!pdf-e.pdf

[2] ETSI, "5G; NR; Multiplexing and channel coding (3GPP TS 38.212 version 16.2.0 Release 16)," *ETSI.org*, 2020. Accessed: Jun. 14, 2024. [Online], Available: https://www.etsi.org/deliver/etsi_ts/138200_138299/138212/16.02.00_60/ts_138212v160200p.pdf

[3] D. Hui, S. Sandberg, Y. Blankenship, M. Andersson, and L. Grosjean, "Channel coding in 5G new radio: a tutorial overview and performance comparison with 4G LTE," *IEEE Vehicular Technology Magazine*, vol. 13, no. 4, pp. 60–69, Dec. 2018, doi: 10.1109/MVT.2018.2867640.

[4] J. Xu, Y. Yuan, and C. Yang, *Channel coding in 5G new radio*. CRC Press, 2022, doi: 10.1201/9781003336174.

[5] T. Richardson and S. Kudekar, "Design of low-density parity check codes for 5G new radio," *IEEE Communications Magazine*, vol. 56, no. 3, pp. 28–34, Mar. 2018, doi: 10.1109/MCOM.2018.1700839.

[6] M. Mensouri and A. Aaroud, "Performance and complexity comparisons of polar codes and LDPC codes," in *Advanced Intelligent Systems for Sustainable Development*, 2020, pp. 207–216, doi: 10.1007/978-3-030-33103-0_21.

[7] D. Čarapić, M. Maksimović, and M. Forcan, "Performance analysis of LDPC and Polar codes for message transmissions over different channel models," in *8th International Conference on Electronics, Telecommunications, Computing, Automatics and Nuclear Engineering-IcETRAN*, 2021, pp. 1–6.

[8] K. W. Jensen, "Polar codes and LDPC codes in 5G new radio," Department of Informatics, University of Bergen, 2022.

[9] B. Tahir, S. Schwarz, and M. Rupp, "BER comparison between convolutional, turbo, LDPC, and polar codes," in *2017 24th International Conference on Telecommunications (ICT)*, May 2017, pp. 1–7, doi: 10.1109/ICT.2017.7998249.

[10] K. D. Rao, "Performance analysis of enhanced turbo and polar codes with list decoding for URLLC in 5G systems," in *2019 IEEE 5th International Conference for Convergence in Technology, I2CT 2019*, Mar. 2019, pp. 1–6, doi: 10.1109/I2CT45611.2019.9033551.

[11] A. M. Cuc, C. Grava, F. L. Morgos, and T. A. Burca, "Performances comparison between low-density parity-check codes and polar codes," in *International Conference on Systems, Signals, and Image Processing*, Jun. 2022, pp. 1–4, doi: 10.1109/IWSSIP55020.2022.9854483.

[12] K. El-Abbasy, R. Taki Eldin, S. El Ramly, and B. Abdelhamid, "Optimized polar codes as forward error correction coding for digital video broadcasting systems," *Electronics*, vol. 10, no. 17, p. 2152, Sep. 2021, doi: 10.3390/electronics10172152.

[13] L. Fanari, E. Iradier, I. Bilbao, R. Cabrera, J. Montalban, and P. Angueira, "Comparison between different channel coding techniques for ieee 802.11be within factory automation scenarios," *Sensors*, vol. 21, no. 21, p. 7209, Oct. 2021, doi: 10.3390/s21217209.

[14] D. Chatzoulis, C. Chaikalis, D. Kosmanos, K. E. Anagnostou, and A. Xenakis, "3GPP 5G V2X error correction coding for various propagation environments: A QoS approach," *Electronics*, vol. 12, no. 13, p. 2898, Jul. 2023, doi: 10.3390/electronics12132898.

[15] M. Sybis, K. Wesolowski, K. Jayasinghe, V. Venkatasubramanian, and V. Vukadinovic, "Channel coding for ultra-reliable low-latency communication in 5G systems," in *2016 IEEE 84th Vehicular Technology Conference (VTC-Fall)*, Sep. 2016, vol. 0, pp. 1–5, doi: 10.1109/VTCFall.2016.7880930.

[16] G.-R. Barb, M. Otesteanu, G. Budura, and C. Balint, "Performance evaluation of TDL channels for downlink 5G MIMO systems," in *2019 International Symposium on Signals, Circuits and Systems (ISSCS)*, Jul. 2019, pp. 1–4, doi: 10.1109/ISSCS.2019.8801790.

[17] A. Gunturu, A. R. Godala, A. K. Sahoo, and A. K. R. Chavva, "Performance Analysis of OTFS Waveform for 5G NR mmWave Communication System," in *2021 IEEE Wireless Communications and Networking Conference (WCNC)*, Mar. 2021, pp. 1–6, doi: 10.1109/WCNC49053.2021.9417346.

[18] A.-M. Cuc, F. L. Morgoș, and C. Grava, "Performance analysis of turbo codes, LDPC codes, and polar codes over an AWGN channel in the presence of inter-symbol interference," *Sensors*, vol. 23, no. 4, p. 1942, Feb. 2023, doi: 10.3390/s23041942.

[19] A. C. Vaz, C. G. Nayak, D. Nayak, and N. T. Hegde, "Performance analysis of forward error correcting codes in a visible light communication system," in *Proceedings of CONECCT 2021: 7th IEEE International Conference on Electronics, Computing and Communication Technologies*, Jul. 2021, pp. 1–5, doi: 10.1109/CONECCT52877.2021.9622633.

[20] A. C. Vaz, C. Gurudas Nayak, and D. Nayak, "Performance comparison between turbo and polar codes," in *Proceedings of the 3rd International Conference on Electronics and Communication and Aerospace Technology, ICECA 2019*, Jun. 2019, pp. 1072–1075, doi: 10.1109/ICECA.2019.8822077.

[21] W. K. Abdulwahab and A. Abdulrahman Kadhim, "Comparative study of channel coding schemes for 5G," in *ICOASE 2018 - International Conference on Advanced Science and Engineering*, Oct. 2018, pp. 239–243, doi: 10.1109/ICOASE.2018.8548806.

[22] S. Shao *et al.*, "Survey of turbo, LDPC, and polar decoder ASIC implementations," *IEEE Communications Surveys and Tutorials*, vol. 21, no. 3, pp. 2309–2333, 2019, doi: 10.1109/COMST.2019.2893851.

[23] Z. B. Kaykac Egilmez, L. Xiang, R. G. Maunder, and L. Hanzo, "The development, operation and performance of the 5G polar codes," *IEEE Communications Surveys and Tutorials*, vol. 22, no. 1, pp. 96–122, 2020, doi: 10.1109/COMST.2019.2960746.

[24] S. Belhadj and M. L. Abdelmounaim, "On error correction performance of LDPC and Polar codes for the 5G machine type communications," in *2021 IEEE International IOT, Electronics and Mechatronics Conference (IEMTRONICS)*, Apr. 2021, pp. 1–4, doi: 10.1109/IEMTRONICS52119.2021.9422665.

[25] M. H. Khan and G. Zhang, "Evaluation of channel coding techniques for massive machine-type communication in 5G cellular network," in *2020 3rd IEEE International Conference on Information Communication and Signal Processing, ICICSP 2020*, Sep. 2020, pp. 375–379, doi: 10.1109/ICICSP50920.2020.9232037.

[26] ETSI, "5G; Study on channel model for frequencies from 0.5 to 100 GHz (3GPP TR 38.901 version 16.1.0 Release 16)," *ETSI.org*, 2020. https://www.etsi.org/deliver/etsi_tr/138900_138999/138901/16.01.00_60/tr_138901v160100p.pdf (accessed Jun. 14, 2024).

[27] R. G. Gallager, "Low density parity check codes," Sc.D. thesis, MIT, Cambridge, 1960.

[28] R. M. Tanner, "A recursive approach to low complexity codes," *IEEE Transactions on Information Theory*, vol. 27, no. 5, pp. 533–547, Sep. 1981, doi: 10.1109/TIT.1981.1056404.

[29] M. P. C. Fossorier, "Quasi-cyclic low-density parity-check codes from circulant permutation matrices," *IEEE Transactions on Information Theory*, vol. 50, no. 8, pp. 1788–1793, Aug. 2004, doi: 10.1109/TIT.2004.831841.

[30] Y. Sun, M. Karkooti, and J. R. Cavallaro, "VLSI decoder architecture for high throughput, variable block-size and multi-rate LDPC codes," in *2007 IEEE International Symposium on Circuits and Systems (ISCAS)*, May 2007, pp. 2104–2107, doi: 10.1109/ISCAS.2007.378514.

[31] M. Ismail, I. Ahmed, J. Coon, S. Armour, T. Kocak, and J. McGeehan, "Low latency low power bit flipping algorithms for LDPC decoding," in *IEEE International Symposium on Personal, Indoor and Mobile Radio Communications, PIMRC*, Sep. 2010, pp. 278–282, doi: 10.1109/PIMRC.2010.5671820.

[32] P. Santini, M. Battaglioni, M. Baldi, and F. Chiaraluce, "Analysis of the error correction capability of LDPC and MDPC codes under parallel bit-flipping decoding and application to cryptography," *IEEE Transactions on Communications*, vol. 68, no. 8, pp. 4648–4660, Aug. 2020, doi: 10.1109/TCOMM.2020.2987898.

[33] S. Z. Xin, B. F. Cockburn, and S. Bates, "Improved iterative bit flipping decoding algorithms for LDPC convolutional codes," in *IEEE Pacific RIM Conference on Communications, Computers, and Signal Processing - Proceedings*, Aug. 2007, pp. 541–544, doi: 10.1109/PACRIM.2007.4313293.

[34] X.-Y. Hu, E. Eleftheriou, D.-M. Arnold, and A. Dholakia, "Efficient implementations of the sum-product algorithm for decoding LDPC codes," in *GLOBECOM'01. IEEE Global Telecommunications Conference (Cat. No.01CH37270)*, 2001, vol. 2, pp. 1036-1036E, doi: 10.1109/GLOCOM.2001.965575.

[35] J. Chen and M. P. C. Fossorier, "Density evolution for two improved BP-based decoding algorithms of LDPC codes," *IEEE Communications Letters*, vol. 6, no. 5, pp. 208–210, May 2002, doi: 10.1109/4234.1001666.

[36] H. Zhang, D. Yuan, and C. X. Wang, "An improved normalized BP-based decoding algorithm for LDPC codes," in *IET Conference Publications*, 2008, no. 545, pp. 223–226, doi: 10.1049/cp:20080977.

[37] S. Y. Chung, T. J. Richardson, and R. L. Urbanke, "Analysis of sum-product decoding of low-density parity-check codes using a Gaussian approximation," *IEEE Transactions on Information Theory*, vol. 47, no. 2, pp. 657–670, 2001, doi: 10.1109/18.910580.

[38] J. Hagenauer, L. Papke, E. Offer, and L. Papke, "Iterative decoding of binary block and convolutional codes," *IEEE Transactions on Information Theory*, vol. 42, no. 2, pp. 429–445, Mar. 1996, doi: 10.1109/18.485714.

[39] J. Zhao, F. Zarkeshvari, and A. H. Banihashemi, "On implementation of min-sum algorithm and its modifications for decoding low-density parity-check (LDPC) codes," *IEEE Transactions on Communications*, vol. 53, no. 4, pp. 549–554, Apr. 2005, doi: 10.1109/TCOMM.2004.836563.

[40] M. K. Roberts and R. Jayabalan, "A modified normalized min - sum decoding algorithm for irregular LDPC codes," *International Journal of Engineering and Technology*, vol. 5, no. 6, pp. 4881–4893, 2013.

[41] M. Rakibul, D. Siam, M. Mostafa, and I. Rahman, "Optimized min-sum decoding algorithm for low-density parity-check codes," *International Journal of Advanced Computer Science and Applications*, vol. 2, no. 12, pp. 168–174, 2011, doi: 10.14569/IJACSA.2011.021225.

[42] H. Li, B. Bai, X. Mu, J. Zhang, and H. Xu, "Algebra-assisted construction of quasi-cyclic LDPC codes for 5G new radio," *IEEE Access*, vol. 6, pp. 50229–50244, 2018, doi: 10.1109/ACCESS.2018.2868963.

[43] E. Arikan, "Channel polarization: A method for constructing capacity-achieving codes for symmetric binary-input memoryless channels," *IEEE Transactions on Information Theory*, vol. 55, no. 7, pp. 3051–3073, Jul. 2009, doi: 10.1109/TIT.2009.2021379.

[44] E. Arikan, "A performance comparison of polar codes and reed-muller codes," *IEEE Communications Letters*, vol. 12, no. 6, pp. 447–449, Jun. 2008, doi: 10.1109/LCOMM.2008.080017.

[45] I. Tal and A. Vardy, "List decoding of polar codes," *IEEE Transactions on Information Theory*, vol. 61, no. 5, pp. 2213–2226, May 2015, doi: 10.1109/TIT.2015.2410251.

[46] K. Niu and K. Chen, "Stack decoding of polar codes," *Electronics Letters*, vol. 48, no. 12, pp. 695–697, 2012, doi: 10.1049/el.2012.1459.

[47] D. Hui, M. Breschel, and Y. Blankenship, "Interleaved CRC for polar codes," in *IEEE Vehicular Technology Conference*, Jun. 2018, vol. 2018-June, pp. 1–5, doi: 10.1109/VTCSpring.2018.8417497.

[48] J. Chen, Y. Chen, K. Jayasinghe, D. Du, and J. Tan, "Distributing CRC bits to aid polar decoding," in *2017 IEEE Globecom Workshops, GC Wkshps 2017 - Proceedings*, Dec. 2017, vol. 2018-Janua, pp. 1–6, doi: 10.1109/GLOCOMW.2017.8269177.

[49] C. Condo, S. A. Hashemi, A. Ardakani, F. Ercan, and W. J. Gross, "Design and implementation of a polar codes blind detection scheme," *IEEE Transactions on Circuits and Systems II: Express Briefs*, vol. 66, no. 6, pp. 943–947, Jun. 2019, doi: 10.1109/TCSII.2018.2872653.

[50] K. Niu and K. Chen, "CRC-aided decoding of polar codes," *IEEE Communications Letters*, vol. 16, no. 10, pp. 1668–1671, Oct. 2012, doi: 10.1109/LCOMM.2012.090312.121501.

[51] S. A. Hashemi, C. Condo, F. Ercan, and W. J. Gross, "On the performance of polar codes for 5G eMBB control channel," in *Conference Record of 51st Asilomar Conference on Signals, Systems and Computers, ACSSC 2017*, Oct. 2017, pp. 1764–1768, doi: 10.1109/ACSSC.2017.8335664.

[52] W. Ryan and S. Lin, "Channel codes," in *Channel Codes: Classical and Modern*, Cambridge University Press, 2009, pp. 1–692, doi: 10.1017/CBO9780511803253.

[53] K. Niu, K. Chen, J. Lin, and Q. T. Zhang, "Polar codes: Primary concepts and practical decoding algorithms," *IEEE Communications Magazine*, vol. 52, no. 7, pp. 192–203, 2014, doi: 10.1109/MCOM.2014.6852102.

[54] C. Seker and M. T. Guneser, "Review of 5G channel models and modelling of indoor path loss at 32 GHz," *American Journal of Computer Science and Engineering Survey*, vol. 9, no. 1, pp. 1–15, 2021.

[55] S. Fenwick, "5G global mobile network experience awards 2022," *Opensignal*, 2022. https://www.opensignal.com/reports/2022/09/global-5g-global-mobile-network-experience-awards (accessed Jun. 14, 2024).

[56] S. Fenwick, "5G global mobile network experience awards 2023," *Opensignal*, 2023. https://www.opensignal.com/reports/2023/10/global/5g-global-mobile-network-experience-awards (accessed Jun. 14, 2024).

[57] Spectrum Monitoring Technology Advisors B.V. (SMTA), "Global mobile frequencies database, tracking IMT/5G spectrum licenses," *Spectrummonitoring.com*. https://www.spectrummonitoring.com/frequencies.php/ (accessed Jun. 14, 2024).

[58] ETSI, "5G; NR; Base Station (BS) radio transmission and reception (3GPP TS 38.104 version 16.4.0 Release 16)," *ETSI.org*, 2020. https://www.etsi.org/deliver/etsi_ts/138100_138199/138104/16.04.00_60/ts_138104v160400p.pdf (accessed Apr. 25, 2024).

[59] ETSI, "5G; NR; User Equipment (UE) radio access capabilities (3GPP TS 38.306 version 17.0.0 Release 17)," *ETSI.org*, 2022. https://www.etsi.org/deliver/etsi_ts/138300_138399/138306/17.00.00_60/ts_138306v170000p.pdf (accessed Apr. 05, 2024).

[60] ETSI, "5G; NR; Physical layer procedures for data (3GPP TS 38.214 version 16.2.0 Release 16)," *ETSI.org*, 2020. https://www.etsi.org/deliver/etsi_ts/138200_138299/138214/16.02.00_60/ts_138214v160200p.pdf (accessed May 19, 2024).

BIOGRAPHIES OF AUTHORS

Mikhail Khmelevsky received the B.Eng. and M.S. degrees in electrical engineering from Moscow Aviation Institute, Russia, in 2021 and 2023, respectively. Currently, he is a Ph.D. student at the Department of Telecommunication Engineering, Moscow Technical University of Communications and Informatics, Russia. He can be contacted at email: mihail.hmelevskiy@gmail.com.

Gennady Kazakov holds a Ph.D. in the field of radio-electronic systems from Moscow Aviation Institute, Russia. Currently, he is an associate professor at the Department of Theoretical Radio Engineering, Moscow Aviation Institute. His research interests include communication systems and networks, radio relay and optical information transmission systems, network protocols. He can be contacted at email: jee2@mail.ru.